

## DEVELOPMENT OF IMPROVED CAPABILITIES FOR DEPTH DETERMINATION

Mark D. Fisk<sup>1</sup>, Clinton Conrad<sup>1</sup>, and David Jepsen<sup>2</sup>

Mission Research Corporation<sup>1</sup>, Australian Geological Survey Organization<sup>2</sup>

Sponsored by Defense Threat Reduction Agency

Contract No. DTRA01-00-C-0027

### **ABSTRACT**

The objective of this research is to develop improved procedures and criteria for identification and validation of seismic depth phases. This effort includes: (1) inspection of waveforms for events in the Reviewed Event Bulletin (REB) to determine whether depth phases have been identified properly; (2) evaluation of existing procedures and criteria for depth-phase validation; (3) development of statistical methods to quantify the moveout of pP-P and sP-P, accounting for timing uncertainties; (4) investigation of techniques to improve depth-phase identification (i.e., F-detector, optimal frequency/filtering tool, and the relative amplitude (RAMP) technique as a test of whether teleseismic P and depth phases fit a double-couple mechanism); and (5) implementation, testing, evaluation, and delivery of software capabilities for improved depth-phase identification and validation to the Center for Monitoring Research (CMR).

We have implemented a method to compute confidence intervals of pP-P and sP-P moveout. We have applied it to 1342 REB events with observed depth phases to determine the percentage of such events with a 90% confidence interval of moveout greater than various thresholds (e.g., 0.0, 1.0, 1.5 seconds). The results indicate that this method is more effective for determining whether depth phases exhibit moveout than requiring the time difference of pP-P at the nearest station beyond 25 degrees and the farthest station within 100 degrees be greater than 1.5 seconds, a criterion currently used at the CMR. Specifically, 425 of 1342 events (32%) have positive moveout at the 90% confidence level, while 281 of 1342 events (21%) satisfy the latter criterion. In addition, we have found that the moveout confidence intervals are more robust to phase timing errors. For many REB depth-phase events, a limited number of observed depth phases and significant scatter in the pP-P and sP-P travel-time differences often cause the moveout confidence intervals to be too large to confidently determine that the moveout is greater than a given threshold. Also, the overwhelming majority of REB events (about 88%) do not have any associated depth phases. To increase the number of detected depth phases and reduce the scatter associated with timing errors, we have investigated the utility of the F-detector (e.g., Blandford, 1974), a signal processing technique that dramatically amplifies signals that are correlated among array elements, while suppressing uncorrelated noise. Using statistical properties of the F-detector, a probability trace (i.e., time series) may be computed indicating whether filtered signals are significantly correlated across an array at a given time. Preliminary results indicate that the F-detector finds many depth phases that were missed by analysts and may provide a more objective approach for determining onset times of P, pP, and sP. We have also found, as in previous studies of the F-detector, that the frequency bands must be tuned for a given array to account for its aperture and ambient noise characteristics. We have also applied the Relative Amplitude (RAMP) algorithm (e.g., Pearce et al., 1988) to REB events with observed depth phases to determine whether relative amplitudes of teleseismic P, pP, and sP are consistent with double-couple focal mechanisms. We present results of these applications and describe plans to complete these investigations and develop appropriate capabilities into operational analysis tools.

**KEY WORDS:** seismic, depth phases, moveout, F-detector, relative amplitude technique, RAMP

## **OBJECTIVE**

The overall objective of this work is to develop improved procedures and criteria for identification and validation of seismic depth phases. Initial tasks involve inspection of waveforms for REB events to determine whether depth phases were picked properly, and evaluation of the provisional procedures and criteria for depth-phase validation that are currently used at the IDC, based on recommendations by the IDC Technical Experts on Seismic-Acoustic Event Screening in May 1999 (CTBT/WGB/TL-2/31). The main objective of these tasks is to assess where significant improvements, relative to existing capabilities, are needed and can be made. The third main task is to develop a robust statistical method to quantify the moveout of pP-P and sP-P travel time differences, providing rigorous treatment of the number of observed depth phases, their distance range, and the uncertainties in phase onset times. The fourth task is to investigate methods to increase the number of detected depth phases and to validate candidate depth phases relative to a physical model. Research in this area focuses on use of the F-detector (e.g., Blandford, 1974), as a technique to detect more depth phases, and on the relative amplitude (RAMP) technique (e.g., Pearce et al., 1988) to test whether relative amplitudes of teleseismic P, pP, and sP fit a double-couple focal mechanism. The last main task is to implement, test, evaluate, and deliver software tools for improved identification and validation of depth phases to the CMR.

## **RESEARCH ACCOMPLISHED**

### ***Evaluation of REB Depth Solutions***

We have evaluated the existing depth screening procedures and criteria used at the PIDC. Let  $D$  be the depth estimate and  $s_{zz}$  be the variance of the depth estimate in the REB. An event is screened out based on depth if

$$D - 2\sigma_D > 10 \text{ km}, \text{ where } 2\sigma_D = 2\sqrt{s_{zz}} + k.$$

This criterion is equivalent to requiring that a one-sided 97.5% confidence interval of the event focal depth is deeper than 10 km. The term  $k$  is included in the overall depth uncertainty as an interim measure to compensate for model errors that are not adequately represented by  $s_{zz}$ . A value of  $k = 20$  km is used for free-depth solutions. A value of  $k = 0$  km is used for events that satisfy the following depth-phase criteria:

- The signal-to-noise (coda) ratio of the depth phases must be at least 2.0;
- At least three depth phases (of the same type) must be observed for an event (i.e.,  $\text{ndp}(\text{pP}) \geq 3$  and/or  $\text{ndp}(\text{sP}) \geq 3$ );
- The moveout of pP-P travel times, for stations in the distance range of 25 to 100 degrees, is greater than or equal to 1.5 seconds and/or 1.3 seconds for sP-P; and
- The travel time difference,  $T(\text{pP-P}) > 12.9$  seconds and/or  $T(\text{sP-P}) > 19.0$  seconds at the nearest station beyond 25 degrees.

We first examined how many REB events are screened out by the depth screening criteria, using a sample of 5412 REB events above mb 3.5 during July to December 1999. Figure 1 depicts the results. The left panel shows histograms of 2228 events (about 41%) with unconstrained depth estimates (white bars), 1079 events (about 20%) that are screened out by depth (green bars), and 128 events (only about 2%) that satisfy the depth-phase criteria listed above (blue bars). The right panel shows 661 REB events above mb 3.5 with depth-phase solutions (white bars) and the 128 events that satisfy the depth-phase criteria.

We also examined the validity of the REB depth confidence intervals using comparisons to other published depth solutions that are thought to be reliable and independent. For example, Figure 2 (left panel) shows REB free-depth estimates versus PDE (Preliminary Determination of Epicenters) depth-phase solutions, published by the U.S. National Earthquake Information Center (NEIC) for 1086 common events above mb 3.5. Using  $k = 20$  km, only three REB depth confidence intervals are significantly deeper than the corresponding PDE depth estimates. Thus, 99.7% of the REB confidence intervals are consistent with or

shallower than the PDE depth-phase solutions, and none of the events that are shallower than 10 km, according to the PDE, are screened out based on the REB free-depth solutions. Similar comparisons were made of REB depth confidence intervals to depth estimates published by the Japanese Meteorological Agency (JMA), the Chinese National Data Center, and the Southern California Earthquake Center (see Fisk et al., 2000). Using over 1600 events, 99.8% of the REB free-depth confidence intervals are consistent with or shallower than the corresponding depth estimates in the other bulletins.

We also examined REB depth-phase solutions, including a comparison of 903 common events with depth-phase solutions reported in both the REB and PDE. Figure 2 (right panel) shows that the REB and PDE depth-phase solutions generally compare quite well, although several events were examined for which the analysts misidentified depth phases that used to obtain the REB depth estimates. In some cases, the depth-phase criteria (defined above) were not satisfied; hence, these events were not screened out. However, we have found several cases with invalid depth phases for which the depth-phase criteria were satisfied.

These evaluation results indicate significant room for improvement in the performance and robustness of the depth screening criteria, especially with regard to the detection and analysis of depth phases. This motivates the focus of our efforts on methods to detect more depth phases and better validate them.

### ***Confidence Intervals of Depth-Phase Moveout***

We have developed a method for computing confidence intervals of the moveout of pP-P and sP-P travel-time differences. The method, based on the  $t$ -distribution, provides rigorous treatment of the number, distance range, and timing uncertainties of observed depth phases. We have applied this method to a sample of 1342 REB events with observed depth phases to determine the percentage of events that exhibit positive moveout at the 90% confidence level. We have compared the results to those based on the IDC depth-phase criteria, as shown in Figure 3, where the black bars represent the 1342 events with depth phases, binned by depth in 10 km intervals, and the green bars represent the numbers of events that satisfy the alternate depth-phase criteria. The left panel shows that 281 events (about 21%) are screened out by the current IDC criteria, while the right panel shows that 425 events (about 32%) are screened out if we require 90% confidence of positive moveout and  $T(\text{pP-P}) > 6.1$  seconds for the nearest measurement beyond 25 degrees. The additional events that are screened out by the latter set of criteria are primarily between 20-40 km deep.

In general, we have also found that the confidence intervals provide a more robust approach for determining whether depth phases exhibit moveout than the current IDC moveout criterion of using the time difference of pP-P or sP-P at the nearest and farthest stations in the distance range of 25 to 100 degrees. For example, the left panel of Figure 4 shows an event that satisfies the IDC moveout criterion because the pP-P time difference between the first and last observations between 25 and 100 degrees is more than 1.5 seconds. However, the scatter and the limited range of the three pP observations do not permit the moveout to be determined accurately. In fact, the 90% confidence interval, depicted by the range of slopes shown (green lines), indicates large uncertainty (including negative values) in the moveout at the 90% confidence level. Alternatively, the right panel of Figure 4 shows an example of an event that does not satisfy the IDC moveout criterion because the first and last measurements of pP-P do not have a time difference of 1.5 seconds. However, the 90% confidence interval of pP-P moveout is entirely positive. The moveout of the event on the right is better constrained, based on the number and distance range of the depth phases; thus, it is a better candidate for screening by depth phases. These results show that requiring 90% confidence of positive moveout is a more robust criterion, and more effective, than the current IDC moveout criterion.

### ***Application of the F-detector***

Upon examining many REB events, we found that small numbers of observed depth phases and significant scatter in pP-P and sP-P travel-time differences often cause the 90% confidence intervals of moveout to be too large to confidently determine that the moveout is positive. We have also found that it is often difficult to detect and objectively pick onset times for many depth phases if they are emergent and have significant P coda preceding them. This motivated us to investigate the utility of the F-detector to detect more depth phases and objectively/consistently determine their onset times, so that moveout confidence intervals can be determined more precisely, allowing more events with depth-phase solutions to be screened out.

The F-detector is a signal processing technique (e.g., Blandford, 1974) that dramatically amplifies signals that are correlated among array elements, while suppressing uncorrelated noise and/or spikes on individual element. The algorithm first forms a beam (i.e., a stacked average of signals from the array elements, aligned to the event epicenter). The beam is bandpass-filtered and smoothed over a time window. It is then divided by the difference of this quantity and the average individual channel power, filtered in the same passband and smoothed over the same time window. If the signal is highly correlated among array elements, this ratio, defined as  $F$ , will be large. Alternatively, the expected value of  $F$  is unity for equal, uncorrelated noise on all channels. Assuming uncorrelated Gaussian noise,  $F$  has a non-central F-distribution, which allows a probability to be computed of whether the array signals are significantly correlated at any given time.

Figure 5 shows an example of how the F-detector can help identify depth phases for ASAR (Alice Springs, Australia) recording of an mb 3.6 event near the Lop Nor test site on 4 February 2001. Shown from bottom to top is the array beam, filtered in the 2.0-4.0 Hz band, the value of  $F$  as a function of time (F-trace), the probability trace, and the derivative of the probability trace with respect to time. Also shown are the P and pP arrivals in the REB, the IASPEI91 predicted pP and sP arrival times (labeled pX and sX), and the onsets of P, pP, and sP, based on the F-detector (labeled p1, p2, p3 in the top panel). The F-trace increases near the onset of the P, pP, and sP phases, where the array signals become well correlated. The probability trace clearly shows onset of P, pP, and sP phases at times close to their theoretical values.

Figure 6 shows the travel-time differences of pP-P (green circles) and sP-P (blue squares) for the same event on 4 February 2001. The solid lines represent least-squares fits to the moveout data and the dotted lines represent the predicted moveout, based on IASPEI91. The left panel shows the depth phases associated in the REB (pP only), while the right panel shows the depth phases that were identified using the F-detector (pP and sP), including additional depth phases at CMAR. Note that the 90% confidence interval of the pP-P moveout for the REB solution is not entirely greater than zero; hence, this event would not be screened out. However, the F-detector results on the right show that the 90% confidence intervals of pP-P and sP-P moveout are both entirely greater than zero. Thus, the additional depth phases obtained from the F-detector provide sufficient evidence of valid depth-phase moveout, which could allow this event to be screened out.

We have applied the F-detector to seven events near the Lop Nor test site since 1 January 1999. All of these events have relatively shallow REB depth-phase solutions (i.e., less than 30 km deep), none of which satisfy the IDC moveout criterion. After applying the F-detector, 5 of the 7 events have 90% moveout confidence intervals that are positive, providing evidence of valid depth-phase solutions for these events. We also applied the F-detector to a global sample of 136 REB events with depth-phase solutions between 50 and 100 km deep. The F-detector found 49 additional (high-confidence) depth phases that were not in the REB.

As in previous studies of the F-detector (e.g., Blandford, 2000; Bowers, 1999), we have found that the frequency band(s) must be tuned for a given array to account for the array aperture and ambient noise characteristics. For some small-aperture arrays, we find that noise can be significantly correlated between array elements (e.g., noise from the North Sea at ARCES), causing the F-trace to be large even when no signal is present. However, it is typically possible to diminish the effects of correlated noise by filtering in a particular frequency band. For example, we found that the 3.0-6.0 Hz band typically works well for small aperture arrays (such as ARCES and FINES), while the 0.5-3.0 Hz band typically works better for larger aperture arrays (such as YKA and CMAR). We plan to examine the effects of different frequency bands for various arrays to optimize the performance of the F-detector for identifying depth phases.

We have also found that the probability trace can saturate to unity, particularly for large events, following the onset of the P phase. This is because the P coda can be sufficiently correlated, obscuring signals from pP or sP phases in the probability trace. One way to enhance the signals of depth phases in this situation is to increase the threshold value used to calculate the probability trace, which corresponds to assuming a greater signal-to-noise ratio. This increases the value of  $F$  at which the probability trace saturates, making depth phases more prominent on the probability trace. Blandford (2000) has also suggested dividing  $F$  by its long-term average to improve its detection performance.

### ***Application of the Relative Amplitude (RAMP) Technique***

To validate depth phases by a physical model, we have investigated the utility of the Relative Amplitude (RAMP) technique (e.g., Pearce et al., 1988). RAMP searches a strike-slip-dip parameter space using relative amplitudes and polarities of P, depth phases, and/or 3 components of S phases at a number of stations to determine the range of moment tensor solutions that are consistent with the input data. In our application of RAMP, we restricted the parameter space to double-couple solutions consistent with P, pP, and sP amplitudes measured in observed and predicted windows and filtered in the 0.6 to 4.0 Hz band. A 5x5x5 degree strike-slip-dip grid was used, with a total of 93312 possible solutions. This grid size allows RAMP to process quickly while being dense enough so that solutions can be formed. We did not use the polarities because they are often difficult to determine confidently. As a result, this allowed many more solutions to form, of which many were redundant. Since the amplitudes can be affected by attenuation (particularly along the two-way depth-to-surface path), seismic noise, complex pulse shape, interfering arrivals, and instrument response, we imposed a 33% uncertainty on the amplitudes to encompass these variations. If small uncertainties are imposed, RAMP will often fail to form events. Alternatively, if the uncertainty is too large, the events may not form well-constrained solutions. We further allow incompatible relative amplitudes at one station, so that a potentially valid solution is not excluded due to anomalous amplitudes at a single station. Last, a simple attenuation model is used, with  $Q_\alpha = 250$  and  $Q_\beta = 100$ .

We applied this version of RAMP to 661 REB depth-phase solutions during July to December 1999, of which 434 events have depth estimates less than 50 km. Note that none of these 434 events satisfy the IDC depth-phase screening criteria. Figures 7 and 8 show examples of waveforms (left) and RAMP solutions (right) for events in the Indian Ocean and South Africa, respectively. Observed depth phases in the REB are labeled as pP and sP, while predicted depth-phase arrivals are labeled as pX and sX. Maximum amplitudes of these phases are calculated in a 3-second time window about these positions. The grids in Figures 7 and 8 represent the slip (across) and dip (down) solution space, with the orientation of the arrow (clockwise) indicating the strike. We consider the Indian Ocean event, with 23 solutions, to be well constrained, and the South African event, with 2024 solutions, to be poorly constrained. Note that the solutions are divided into mirrored regions as a result of not constraining the polarities of the phases.

Of the 661 events, 104 were not compatible with any double-couple solution, while 557 were. Of these, 281 events have 500 or fewer solutions (corresponding to about 0.5% of the parameter space), which we consider to be well constrained. Of the 434 events with REB depth-phase solutions less than 50 km deep, 186 have well-constrained mechanisms, and could potentially be screened out. Although further work is needed, incorporating the use of RAMP to screen out events with well-constrained double-couple solutions could more than double the screening performance based on depth phases. It also has the advantage that the depth phases would be validated by a physical model.

### **CONCLUSIONS AND RECOMMENDATIONS**

The main results obtained thus far under this contract are as follows. First, evaluation of the performance of the IDC depth screening criteria indicates that the criteria are quite conservative and that only about 2% of the events above mb 3.5 in the REB satisfy the depth-phase criteria. Thus, identification of more valid depth phases appears to be the best way to significantly improve event screening (or discrimination) based on depth. Second, the confidence-interval approach we developed is more robust and more effective for testing whether observed depth phases for an event exhibit moveout than the existing moveout criterion currently used at the IDC. The former approach was found to improve the screening performance (32% as compared to 21%) for 1342 REB depth-phase solutions that were examined. Also, numerous cases were found for which the IDC moveout criterion does not properly account for uncertainties in the estimated moveout based on the number, distance range, and timing errors of observed depth phases, while the confidence intervals of moveout do provide rigorous treatment of these factors. Third, we found that the F-detector can help identify many more depth phases, which can help to determine confidence intervals of moveout more precisely, thereby confirming valid depth-phase solutions. Fourth, RAMP can validate depth-phase solutions by fitting relative amplitudes of P, pP, and sP phases to double-couple focal mechanisms. We found that RAMP is

particularly useful for relatively shallow events. For example, RAMP obtained “well-constrained” solutions for 186 of 434 REB events (i.e., about 41%) above mb 3.5 with depth-phase solutions shallower than 50 km, while none of these events could be screened out by the current IDC depth-phase criteria.

During the remainder of this contract, we plan to continue to optimize and evaluate these combined capabilities, to identify and validate depth phases for a greater number of events. Specific efforts will focus on tuning the F-detector for IMS seismic arrays, and on evaluating its performance on a larger sample of REB events. We also plan to further evaluate the utility of the RAMP algorithm on a larger set of REB events, including those with and without observed depth phases. We plan to examine effects of using various attenuation models and provide a more rigorous determination of the number of RAMP solutions that defines a well-constrained focal mechanism for a given event, based on theoretical considerations and applications to ground-truth events. We also plan to examine whether events with mis-labelled depth phases or events without actual depth phases (such as explosions) can form well-constrained RAMP solutions. We also plan to examine whether polarities of P and depth phases provide a significant improvement in constraining the RAMP solution space, and the degree to which this imposes additional burden on the analysts. Last, we plan to deliver software capabilities to perform these functions to the CMR.

## **REFERENCES**

- Blandford, R. R. (1974). An automatic event detector at the Tonto Forest seismic observatory, *Geophysics*, **39**, 633-643.
- Blandford, R. R. (2000). Private communication.
- Bowers, D. (1999). Depth Phase Identification for Event Screening: Future Improvements, in *Proceedings of the IDC Technical Experts Meeting on Seismic-Acoustic Event Screening*, 21-25 May 1999.
- CTBT/WGB/TL-2/31 (1999). Report of the IDC Technical Experts Meeting on Seismic-Acoustic Event Screening, 21-25 May 1999.
- CTBT/WGB/TL-2/58 (2001). Report of the IDC Technical Experts Meeting on Seismic-Acoustic Event Screening, 10-14 November 2000.
- Fisk, M. D., D. Jepsen, and J. R. Murphy (2000). Experimental Seismic Event-Screening Criteria at the Prototype International Data Center, submitted to *Pure and Applied Geophysics (PAGEOPH) Special Volume on Seismic Event Discrimination and Identification Related to Monitoring a Comprehensive Test-Ban Treaty (CTBT)*.
- Jepsen D. and M. D. Fisk (1999). Evaluation of PIDC Seismic Depth Estimates and Uncertainties, in *Proceedings of the IDC Technical Experts Meeting on Seismic-Acoustic Event Screening*, 21-25 May 1999.
- Pearce, R. G., J. A. Hudson and A. Douglas (1988). On the use of P-wave seismograms to identify a double-couple source, *Bull. Seism. Soc. Am.*, **78**, 651-671.

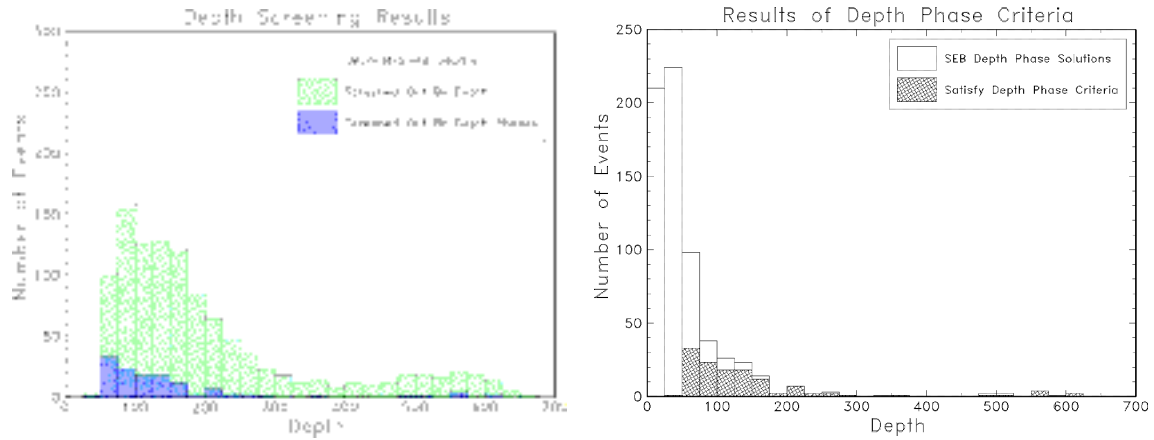


Figure 1. The left panel shows histograms of 2228 REB events above mb 3.5 with unconstrained depth estimates (white bars), 1079 events that are screened out by depth (green bars), and 128 events that satisfy the IDC depth-phase criteria (blue bars). The right panel shows 661 REB events above mb 3.5 with depth-phase solutions (white bars) and the 128 events that satisfy the IDC depth-phase criteria. Only about 2% of the REB events have depth phases that satisfy the IDC depth-phase criteria.

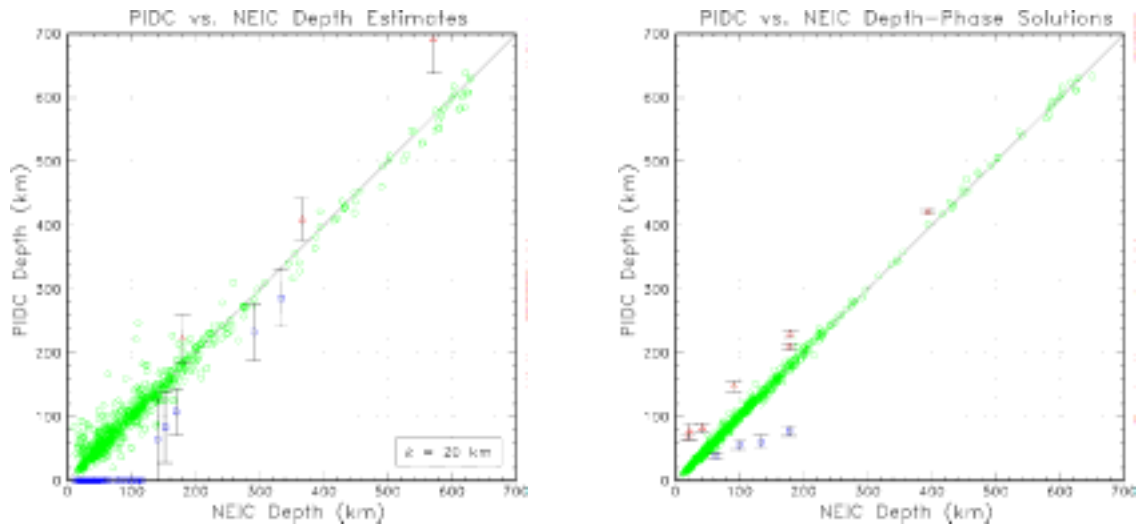


Figure 2. Comparisons of PIDC and NEIC depth estimates for common events above mb 3.5. REB depth confidence intervals are shown only for events with 97.5% confidence intervals that do not contain the NEIC depth estimate. The left panel compares 1086 PIDC free-depth solutions to corresponding NEIC depth-phase solutions; 99.7% of the PIDC free-depth solutions are consistent with or shallower than the NEIC depth-phase solutions. The right panel compares 903 PIDC and NEIC depth-phase solutions; 99.2% of the PIDC depth-phase solutions are consistent with or shallower than the NEIC depth-phase solutions. The seven REB events with depth-phase solutions that are significantly deeper than the corresponding NEIC depth estimates were examined in detail and found to have erroneous depth-phase picks in the REB.

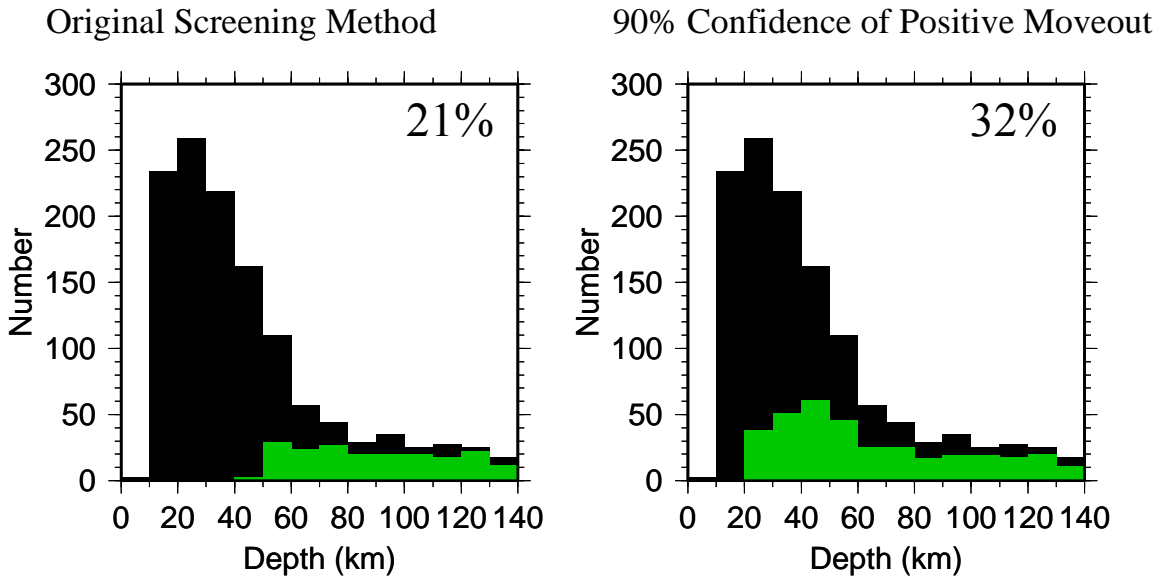


Figure 3. Histograms of 1342 REB events with depth phases (black) and those that satisfy alternate depth-phase criteria (green). The left panel shows the results using the IDC depth-phase criteria, while the right panel shows the results for events with a 90% confidence interval of moveout that is entirely positive, and the pP-P travel-time difference of more than 6.1 seconds at the nearest station beyond 25 degrees.

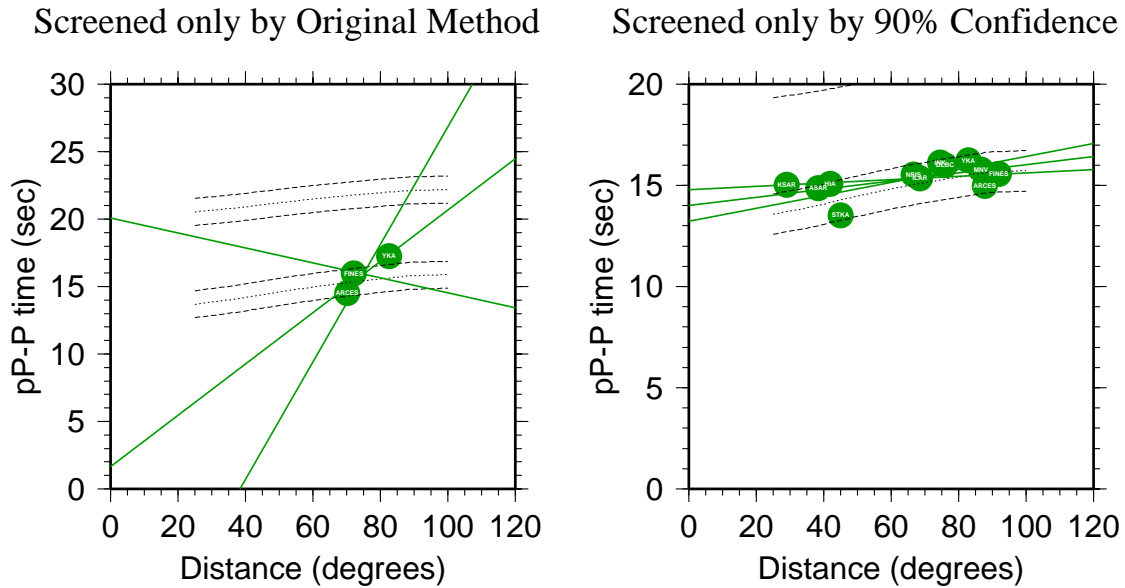


Figure 4. Comparison of alternate moveout criteria for two events with REB depth estimates of 54 km. The event on the left (orid=20336863) satisfies the IDC moveout criterion ( $>1.5$  seconds between extreme pP-P travel-time measurements), but does not have 90% confidence of positive moveout. The event on the right (orid=20296734) does not satisfy the IDC moveout criterion, but does have 90% confidence of positive moveout. Solid lines represent least-squares fits to the data and the range of slopes at the 90% confidence level. Dotted lines are the pP-P travel-time differences predicted by IASPEI91 and  $\pm 1$  second residuals.



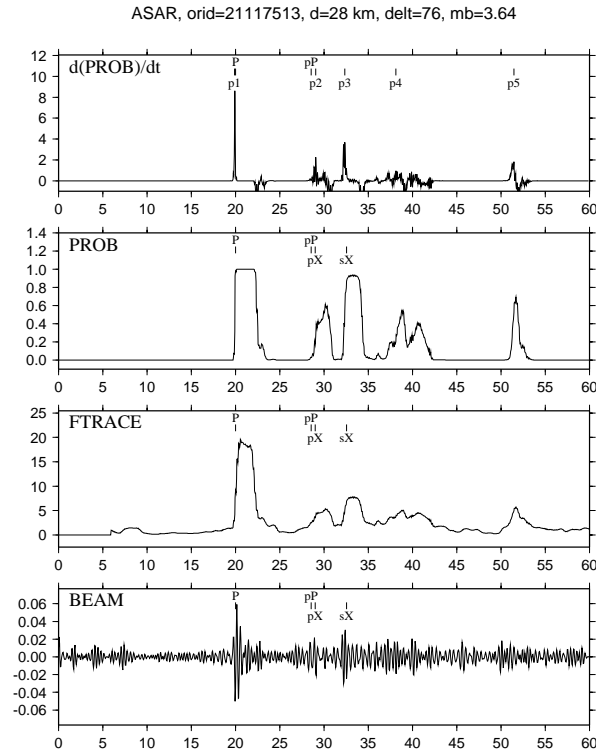


Figure 5. F-detector results for ASAR recording of an mb 3.6 event near Lop Nor on 2001/02/04. Shown from bottom to top are the beam in the 2.0-4.0 Hz band,  $F$  as a function of time, the probability trace, and derivative of the probability trace with respect to time. Also shown are the P and pP arrivals in the REB, arrivals predicted by IASPEI91 (pX and sX), and onsets of P, pP, sP (p1, p2, p3) based on the F-detector.

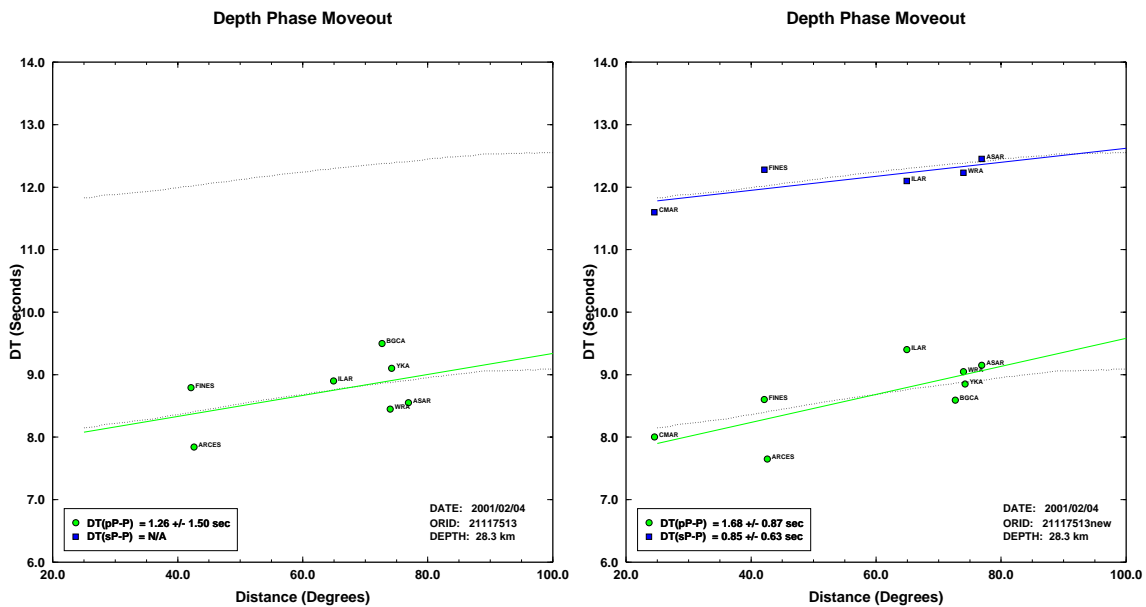


Figure 6. Travel time differences of pP-P (green circles) and sP-P (blue squares) for an REB event near the Lop Nor test site on 4 February 2001. The left panel shows the depth phases associated in the REB, while the panel on the right shows the depth phases that were identified using the F-detector.

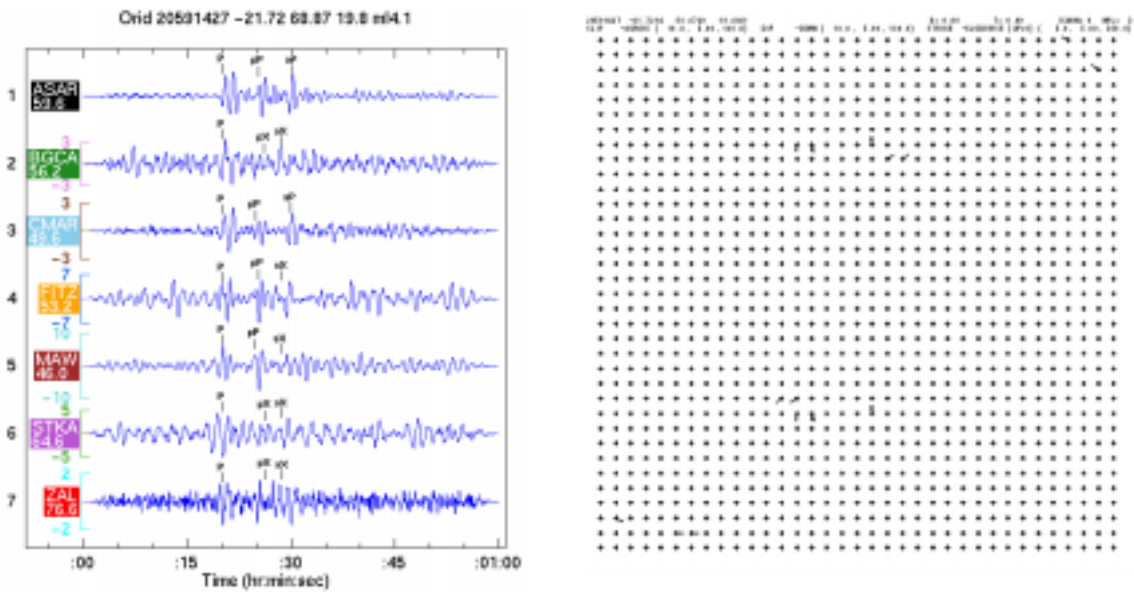


Figure 7. Selected waveforms (left) and the double-couple solutions (right) that are consistent with the relative amplitudes of P, pP, and sP for an Indian Ocean earthquake. This event, with 23 solutions from the RAMP algorithm, is considered to have a well-constrained focal mechanism. The grid represents the slip (across) and dip (down) solution space, with the orientation of the arrow (clockwise) indicating the strike.

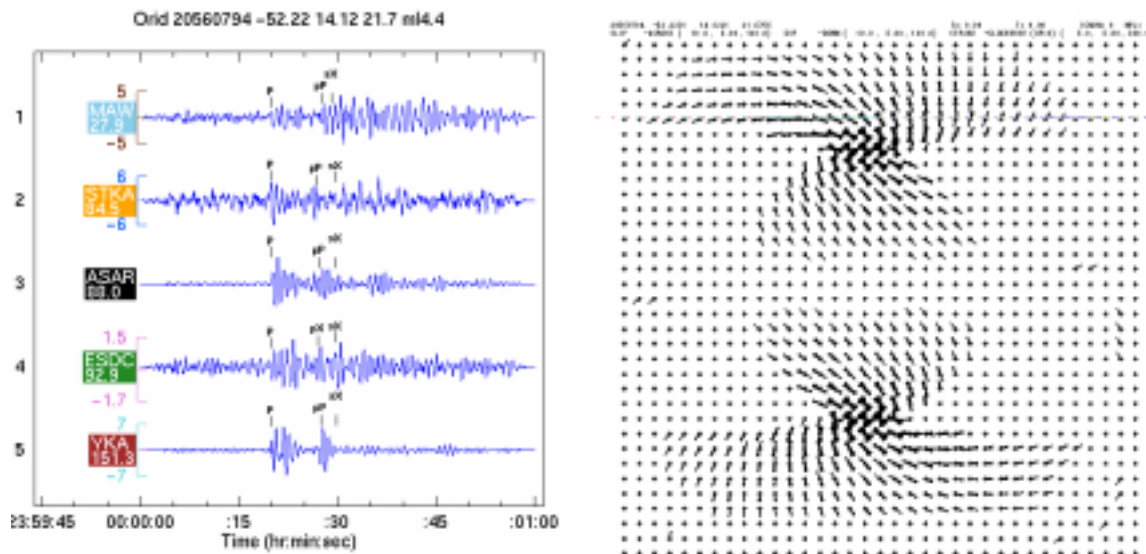


Figure 7. Selected waveforms (left) and the double-couple solutions (right) that are consistent with the relative amplitudes of P, pP, and sP for a South African earthquake. This event, with 2024 solutions from the RAMP algorithm, is considered to have a poorly-constrained focal mechanism.